Part I
Control of Cell/Film Interactions

Layer-by-Layer Films for Biomedical Applications, First Edition.
Edited by Catherine Picart, Frank Caruso, and Jean-Claude Voegel.

1
Controlling Cell Adhesion Using pH-Modified Polyelectrolyte Multilayer Films

Marcus S. Niepel, Kristin Kirchhof, Matthias Menzel, Andreas Heilmann, and Thomas Groth

1.1
Introduction

The majority of cells in our body are organized in tissues, where cell–matrix and cell–cell adhesions are important determinants of their function. Adhesion of mammalian cells to the extracellular matrix (ECM) is regulated mainly by integrins that represent not only anchoring functions but also two-directional signaling machines [1]. Signal transduction processes induced by ligation of integrins to ECM proteins such as collagens (COLs), fibronectin (FN), laminin, and others lead to intracellular phosphorylation of a plethora of proteins that regulate cell spreading, motility, growth, differentiation, and survival [2]. Hence, adhesion of cells on foreign surfaces has been studied for decades to understand how properties of material surfaces affect cell behavior [3–5]. Adsorption of proteins from surrounding media, but also secreted by cells, and their conformation is dependent on chemical compositions and physical properties of surfaces such as wettability, surface charge, and topography, which affects cell behavior [6–8]. In addition, the ability of cells to organize matrix proteins on surfaces in a fibrillar manner like in the natural matrix seems to be also an important process that is highly dependent on surface properties [9–11]. Therefore, a precise control of surface composition and properties of biomaterials may decide about success or failure of medical interventions with blood linings, implants, artificial organs, and so on.

As discussed in following chapters, the layer-by-layer (LbL) technique was initially developed based on electrostatic interaction and ion pairing of oppositely charged polyelectrolytes (PELs) that are adsorbed alternately onto charged surfaces [12]. However, other forces such as hydrogen bonding also might foster polyelectrolyte multilayer (PEM) assembly as the intrinsic charge of the PEL might be reduced dependent on the environmental conditions [13]. One great advantage of the LbL technique is that PEM properties such as surface charge, wettability, thickness, and viscoelasticity can be tailored by the selection of PEL (molar mass, charge density, chain stiffness) as well as the ambient medium characteristics (pH value, ionic strength, temperature) [12]. Stronger effects on charge and conformation of weak PEL are induced by pH value, whereas strong PEL such as heparin

Layer-by-Layer Films for Biomedical Applications, First Edition.
Edited by Catherine Picart, Frank Caruso, and Jean-Claude Voegel.

(HEP) are less affected. As a result, the adjustment of pH can be used to control PEL conformation as well as adsorption and, thus, the PEM structure and composition [12]. Synthetic PEL are widely used in basic research for biomedical applications and include polyanions such as poly (styrene sulfonate) (PSS, strong PEL) or poly (acrylic acid) (PAA, weak PEL) and polycations such as poly (allylamine hydrochloride) (PAH). Linear growing PSS/PAH multilayers are most frequently used since layer formation can be easily controlled by pH value and ionic strength [14, 15]. PAA/PAH multilayers are another synthetic system, which allows the control of surface topography by pH variation or by posttreatment in acidic solutions [16–18]. In addition, its viscoelasticity can be tuned from rather soft (200 kPa) to highly rigid (142 MPa) surfaces, which influences cellular interaction, too [19]. However, in case of synthetic PEL, initial cell interactions are based on nonspecific physical interaction forces (e.g., Coulomb and van der Waals forces) and depend also on nonspecific adsorption of proteins from the surrounding media [20]. Hence, cell behavior on such kind of multilayers is not predictable because adsorption of proteins can be followed by conformational changes that negatively affect the interaction with cells [21, 22].

Cells in tissues are surrounded by and interact with the ECM, a mixture of proteins and polysaccharides (i.e., mainly glycosaminoglycans (GAGs)) that provides mechanical and chemical stimuli to cells. Hence, it seems prospective to use ECM components as or within PEM systems. ECM components used for the assembly of such bioactive PEM are, for example, COL [23], chondroitin sulfate (ChS) [24, 25], gelatine (GEL) [26], HEP [27, 28], and hyaluronic acid (HA) [29, 30]. Since most of these molecules represent polyanions, polysaccharides such as chitosan (CHI) [31, 32], and polypeptides such as poly-L-lysine (PLL) have been used as biocompatible polycations [33]. Since cells possess receptors for proteins such as COL and GAG like HA, and GAG such as HEP specifically bind proteins important for adhesion, growth, and differentiation of cells, multilayers composed of such natural polymers offer unique mechanical and biochemical signals to the cells [23, 30, 34]. It has been shown recently, that PEM formation with polysaccharide-based molecules is highly affected by the charge of GAG. Hence, multilayer composition and thickness can be tuned by pH value and ionic strength of the PEL solution [35, 36]. Thereby, the film thickness increases if the pH value of the adsorbing PEL is close to its pK_a value or the ionic strength increases within a narrow range [35, 37]. Moreover, hydration and swelling properties of PEM films are affected, too [38]. Interesting and important to note is that local interactions within the PEM during multilayer formation are probably dependent on the nature of PEL that form the outermost layer, as shown by Xie and Granick [39]. There, the ionization of weak PEL inside multilayers was dependent on the nature of the outer layer, when interacting with strong PEL. As a result, the ionization of weak PEL is changing upon contact with subsequent PEL, which results in variations in corresponding film characteristics such as thickness, hydration, and mechanical properties [40]. These minute variations can influence subsequent events such as protein adsorption as well as controlled release of bioactive molecules such as growth factors and cell interactions [29].

In conclusion, the LbL technique is an effective and rather simple method to tailor not only the viscoelasticity and other biomaterial surface properties but also the biocompatibility of materials intended to be used for biomedical applications. Moreover, these properties can be fine-tuned, changing the environmental conditions such as pH value, ionic strength, and so on, during PEM formation. Here, we focus on how the pH value of PEL solutions influences layer growth and surface properties such as wettability, charge, and topography of two similar PEM systems. Further, we show that a control of the solution pH value directly from the beginning or at later stages of the PEM assembly leads to distinct surface characteristics that affect adhesion and growth of different mammalian cells.

1.2 Influence of pH-Modified PEM Films on Cell Adhesion and Growth

We have studied here particularly surface properties such as wettability and zeta potential of two different pairs of PEL and the effect of film composition on adhesion and growth of mammalian cells. The two multilayer systems were fabricated at either acidic (pH 5.0) or alkaline (pH 9.0) pH value. In both PEM systems, the GAG HEP was used as strong polyanion while either the biopolymer CHI or the synthetic polymer poly(ethylene imine) (PEI) was used as polycation. The film growth and surface properties of each system (HEP/CHI and PEI/HEP) as well as the effect of film composition and pH value during PEM formation on cellular behavior are discussed in the following sections.

1.2.1 HEP/CHI Multilayers

HEP belongs to the group of heterogeneous, linear, anionic GAG. Due to the large amount of negatively charged functional groups such as sulfate monoesters, carboxyl groups, and sulfamido groups, it can be considered as strong polyanion, which means that charge and conformation are independent of a wide range of solution pH value [41]. HEP used here was derived from porcine intestinal mucosa and, according to the manufacturer, has a molecular weight distribution of $M_w \sim 8-25$ kDa. The polycation CHI is prepared by deacetylation of chitin and has a molecular weight of $M_w \sim 500$ kDa with a deacetylation degree of 87.5%. CHI is soluble in water only below pH values of 6.0–6.5, which leads to protonation of amino groups and hence better solubility [42]. The synthetic polymer PEI ($M_w \sim 750$ kDa) was used here as priming layer to obtain a positive charge and appropriate bonding to the sample surfaces, which were either cleaned glass cover slips or gold sensors that were pretreated with mercaptoundecanoic acid (MUDA) to achieve a negative surface charge similar to glass [43]. Both CHI and PEI can be considered as weak polycations meaning that their charge and conformation are dependent on the pH value of the solutions [44]. All PEL were dissolved in 140 mM sodium chloride solution at a concentration of 2 mg ml^{-1}. The pH value of each

solution was controlled directly from the start of the PEM formation and adjusted to either pH 5.0 (denoted as PEM-5) or pH 9.0 (denoted as PEM-9) for the HEP and PEI solutions. Further, the CHI solution was always adjusted to pH 5.0 due to its pH-dependent solubility. Each layer was rinsed with aqueous solutions of the same pH value. The PEM assembly was terminated after 4.0 or 4.5 bilayers of HEP and CHI formed on top of a PEI priming layer.

Static water contact angle (WCA) measurements were performed with an OCA 15+ device (DataPhysics, Filderstadt, Germany) using ultrapure water as test liquid to investigate the change in wetting properties after PEL adsorption. The advantage of WCA measurements is based on the fact that only the uppermost layer is exposed to the test liquid (i.e., water) while any layers underneath are not involved [45]. Figure 1.1 shows that the deposition of PEI led to less wettable surfaces indicated by the increase of WCA compared to glass. The subsequent exposure of the PEI layer to HEP and CHI at acidic pH 5.0 led to an alternating wetting behavior of the terminating layers, which points to a significant change in the surface composition. Such pronounced change of WCA was not found at alkaline conditions. Here, WCA decreased after adsorption of HEP and remained constant during the next three adsorption steps. Then an alternation of WCA was observed that suggests that the formation of a complete adsorption layer was achieved.

Owing to the fact that pure CHI films are more hydrophobic [46] and HEP films hydrophilic [47], the differences in WCA between HEP and CHI at pH 5.0 indicate the dominance of one respective molecule in the outer regions after each coating step. The charge of CHI as a weak PEL ($pK_a \sim 6.5$) [48] is affected by the pH value of the solvent, hence, the layer formation at acidic conditions should be based on

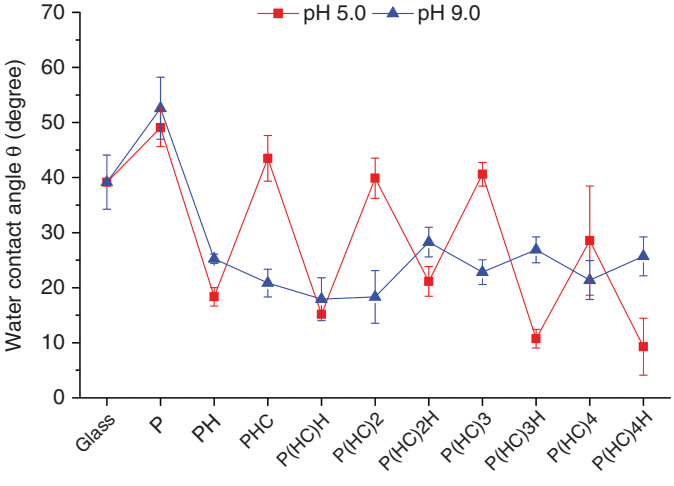

Figure 1.1 Static WCA of PEM consisting of PEI (P), HEP (H) and CHI (C) and assembled at either pH 5.0 (squares) or pH 9.0 (triangles). Mean values and standard deviations of three independent experiments are shown ($n \geq 15$).

ion pairing, since HEP and CHI are both charged and a dominance of either the polyanion or polycation in the terminal layer is achieved [49]. However, the PEM formation at pH 9.0 was quite different. Here, WCA of HEP was shifted to higher values compared to pH 5.0, whereas CHI layers were more hydrophilic than CHI layers at pH 5.0. Since an adsorbed CHI layer becomes deprotonated at pH 9.0, other mechanisms such as hydrogen bonding might be the base for PEM formation, which are weaker than electrostatic interactions, and solution complexation might be favored over surface deposition [50]. The low difference and shifts of WCA of PEM-9 point to a merge of both PEL in the outermost layers.

The results of static contact angle measurements were supported by WCA titration using water with different pH values as test liquid [51]. The titration curves in Figure 1.2a show that HEP layers at pH 5.0 were much more hydrophilic than CHI layers and the WCA rose slightly with increase of pH value, which is probably attributed to the low pK_a value of the sulfate group ($pK_a \sim 0.5-1.5$) [52]. It is interesting to see that WCA of CHI layers increased from pH 2.0 and reached constant values at pH 5.0 (first CHI layer) or pH 4.0 (terminal CHI layer), respectively. The pronounced change of the wetting properties of CHI layers is relatively close to the pK_a value of the CHI amino groups ($pK_a \sim 6.5$) and seems to correspond to changes in charges of the polycation. Others have used contact angle titration to assess the content of charged species in mixed self-assembled monolayers [53]. Here, we can draw the conclusion that PEM-5 possesses a high homogeneity of terminal layers. The WCA titration curves of PEM-9 indicated that layer formation strongly differed from PEM-5 (Figure 1.2b). Terminal CHI layers were much more hydrophilic, even more than the HEP layers, no matter if initial or terminal layer. The WCA of all layers rose up to pH 4.0 reaching an equilibrium thereafter, which could indicate the presence of CHI even in terminal HEP layers. In addition, we speculate that layer formation is distorted at pH 9.0 and solution complexation might be favored since the lower WCA of CHI layers could indicate a higher amount of HEP, which means that the HEP in solution complexes with desorbed CHI from the surface.

In addition to the effect of pH during multilayer formation on their wettability, we studied here the zeta potential of PEM (SurPASS, Anton Paar, Graz, Austria). Typically, a decrease of zeta potential with increasing pH value can be seen due to deprotonation of functional groups and adsorption of hydroxyl ions [54]. As it was deduced already from WCA measurements, the formation of more separated PEM-5 with a dominance of either CHI or HEP in terminal layers should also lead to an alternation of surfaces potential [23, 55, 56]. However, such observation was not made here (Figure 1.3). It was found that zeta potentials of PEM-5 and PEM-9 showed both positive zeta potentials in the acidic and negative potentials in the basic range. This indicates a contribution of both charged species, such as CHI at low and HEP at high pH regions, to the zeta potential, which is also well in line with findings of other groups that not only terminal but also inner layers of PEM contribute to zeta potential [57]. Since these results here contrast observations of other groups where zeta potential was alternating with change of terminal layer

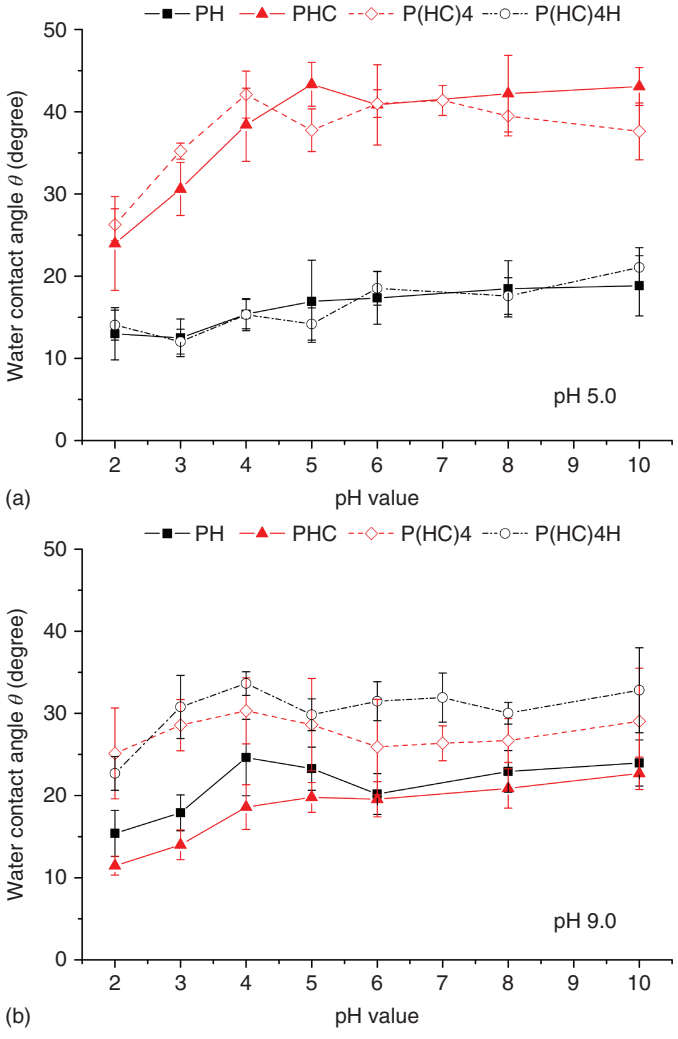

Figure 1.2 Static WCA titration on PEM consisting of HEP and CHI assembled at either pH 5.0 (a) or pH 9.0 (b). Titration curves from pH 2.0 to pH 10 for the first HEP (PH, squares) and CHI layer (PHC, triangles), as well as the terminal CHI ($P(HC)_4$, circles) and HEP layer ($P(HC)_4H$, diamonds) are shown. Values were collected from three independent experiments and mean values and standard deviations were calculated ($n \geq 15$).

[58], it indicates a more swollen nature of PEM based on hydrophilic polysaccharides [57]. It was also surprising to see that a change of terminal layer of PEM-5 did not lead to remarkably different zeta potentials, although WCA measurements indicated a separation of HEP and CHI. This result may be taken as further evidence for a contribution of layers underneath the terminal to zeta potentials. A small difference for both PEM-5 and PEM-9 was a slight shift of point of zero

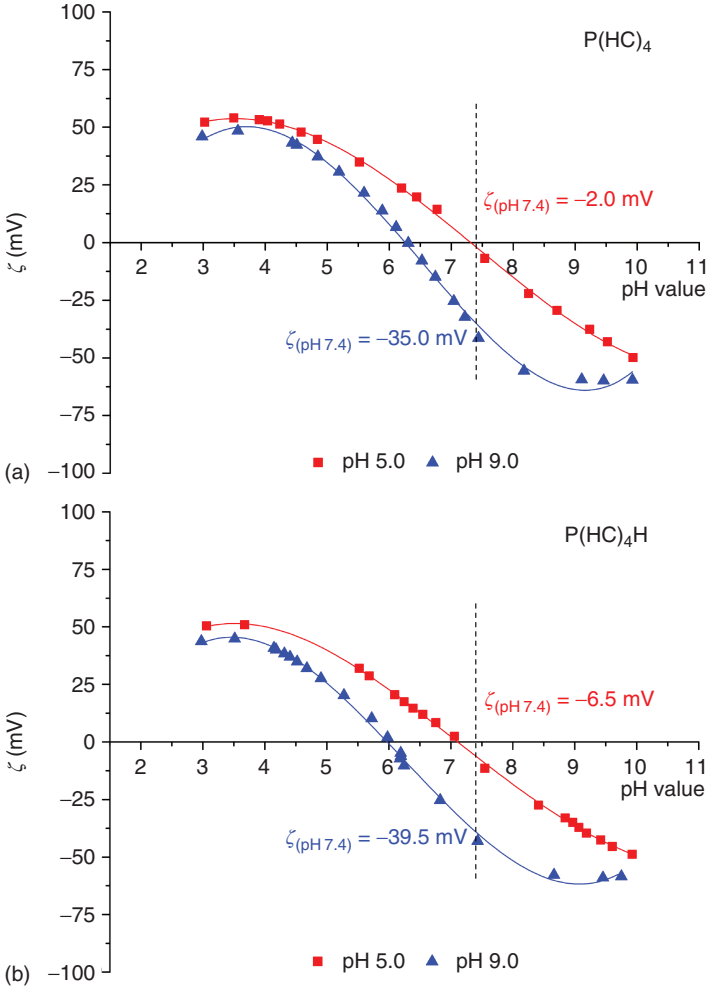

Figure 1.3 Zeta potential titration curves of the terminal CHI (a) and HEP layer (b) assembled at either pH 5.0 (squares) or pH 9.0 (triangles). The pH value of the buffer solution (1 mM potassium chloride) was titrated from pH 10.0 to pH 3.0 with 1 M hydrochloric acid and mean values of four single measurements were calculated.

charge (PZC) to more acidic values when HEP was forming the terminal layer. Lower zeta potentials in the acidic range of PEM-9 could indicate that the glass surface still contributes to the zeta potential, since a larger fraction of HEP would lead to a higher wettability, which was not found in WCA measurements.

PEM formation was also monitored by quartz crystal microbalance (QCM) with additional measurement of damping shifts (ifak, Magdeburg, Germany) and by surface plasmon resonance (SPR) with a Biacore2000 device (GE Healthcare, Little Chalfont, UK). However, SPR measurements were used here to determine the

amount of adsorbed human plasma fibronectin (pFN) onto the terminal PEM. Figure 1.4a shows the frequency shifts of QCM sensors due to the acoustically coupled mass of the respective PEL and its solvent.

The total mass increase during the alternating adsorption of HEP and CHI was higher at acidic than at alkaline conditions, which is indicated by higher frequency shifts here according to Sauerbrey equation [59] (Figure 1.4a). These shifts were always higher for the polycation CHI, which fits to its higher molecular weight [60]. However, the slope of adsorption curves was dependent on the pH

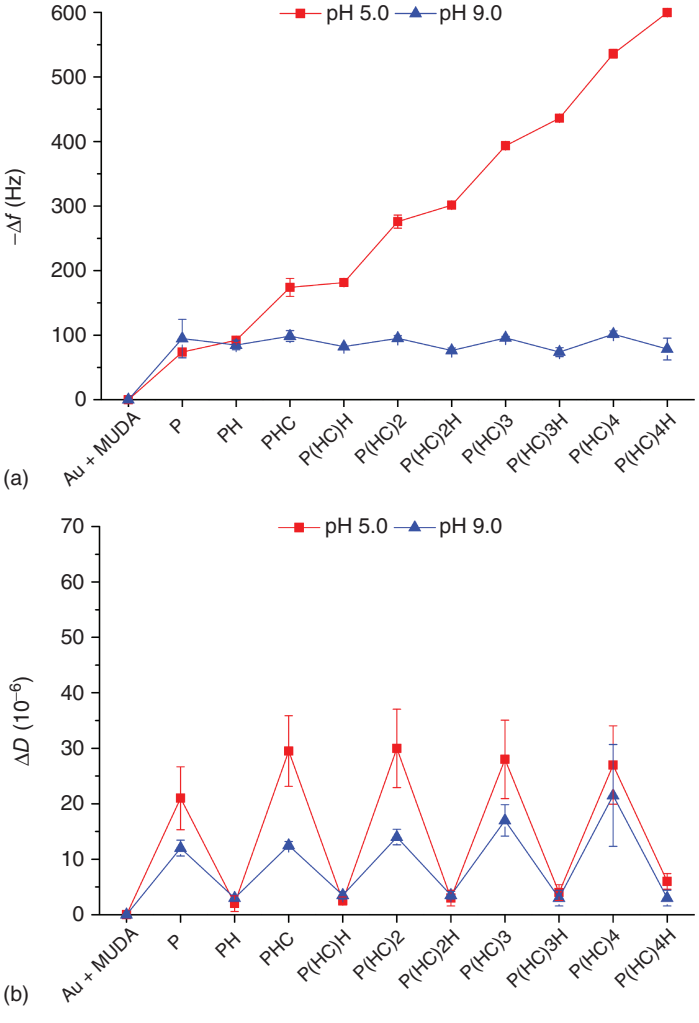

Figure 1.4 QCM measurement of PEM growth. Negative frequency shifts Δf (a) as well as the change in damping ΔD (b) of PEI (P), HEP (H) and CHI (C) multilayers assembled at either pH 5.0 (squares) or pH 9.0 (triangles) are shown. Mean values and standard deviations of measurements performed at room temperature were calculated ($T = 25\,^{\circ}\mathrm{C}$, $n \geq 3$).

value of the PEL solution because the mass increase was almost linear for PEM-5 and remained almost constant for PEM-9. The significant difference in layer mass increase between both pH conditions reflects the different mechanism of complexation of either ion pairing at pH 5.0 [61] and probably hydrogen bonding between amino and hydroxyl groups of adsorbed CHI with HEP sulfate and carboxylic groups at pH 9.0 [50]. In addition, at alkaline conditions, a decrease of PEM mass was observed after HEP adsorption, which was not seen in SPR investigations published elsewhere, where a modest increase in layer mass was observed at pH 9.0 [32]. While SPR measures changes in "dry" layer mass without solvent molecules, QCM detects complete "wet" layer mass and, hence, the solvation of PEL, too. Thus, the water content of the PEM affects the mass of the whole system [58]. Figure 1.4b shows that the damping shift of PEM varied not only with HEP and CHI adsorption but also with the pH value during PEM formation. It is possible that PEI and CHI entrap water within the voluminous architecture, which leads to higher viscoelasticity and, thus, higher damping shifts, but with higher values for acidic conditions because of the much higher mass of PEM. During adsorption of HEP, the smaller molecule might diffuse into the layer structure and displace water molecules, which leads to stiffening and compaction of the PEM along with a decrease in damping [61]. As a result, negative frequency shifts do not necessarily indicate desorption of PEL, since dehydration of the PEM might occur. However, it is also reported that CHI is able to diffuse vertically within the layer architecture, which would cause a rise in water content and, thus, an increase in damping, too [27, 37]. However, in case of HEP/CHI layers assembled at pH 9.0, it could be possible that solution complexation is favored as indicated by the negative frequency shifts. Here, weaker forces such as hydrogen bonding or acid–base interactions might be the driving force that contribute to the layer formation, which has been discussed extensively [61, 62]. Further, CHI is not soluble above pH 6.5 and the ionogenic groups will not be charged at higher pH values. Thus, they cannot contribute to the electrostatic interaction at pH 9.0.

The different character of PEM-9 was also evident by characterization of hydrated PEM with atomic force microscopy (AFM) (NanoWizard®II, JPK, Berlin, Germany) (Figure 1.5). Terminal layers of PEM-5 (a, b) were more homogenous than PEM-9 (c, d). The latter one also showed strong textures that point to island formation. Initial increased adsorption of HEP at pH 5.0 proven by QCM investigations leads to more homogeneous layer formation, which results in highly wettable surfaces, too. However, HEP layers were more textured than CHI layers at acidic conditions, which could be attributed to erosion or solution complexation of the terminal CHI layer. In contrast, layer formation at pH 9.0 is characterized by island formation, which might be related to adsorbed PEI molecules of the priming PEI layer. With increasing layer number, the size of islands could possibly increase and coalesce, which was also described in the literature [60]. Further, the islands point to surfaces that are more inhomogeneous and where still the underlying glass substrate might partly contribute to surface characteristics as shown above.

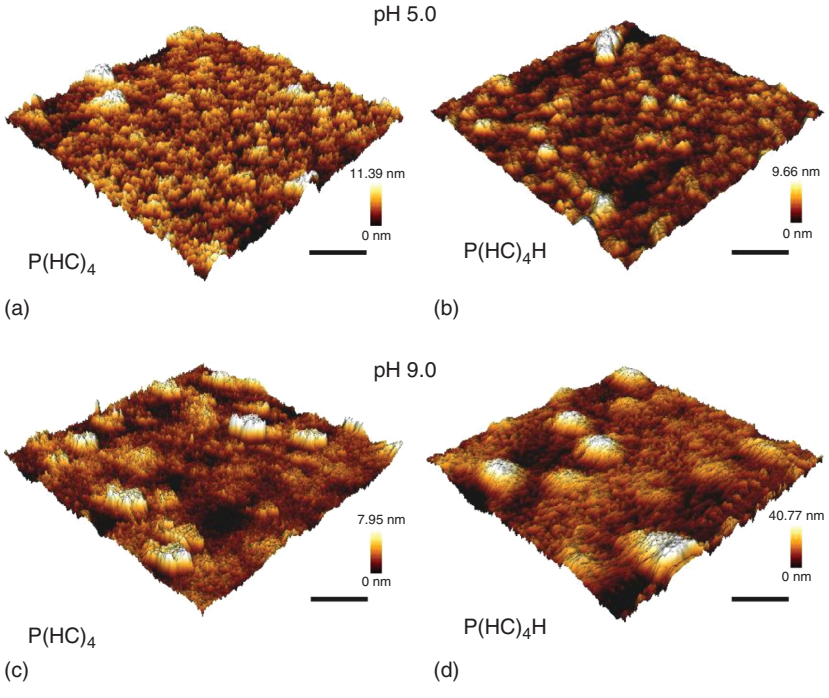

Figure 1.5 AFM images (height profile) of the terminal CHI (a, c) and HEP layer (b, d) in a hydrated state and assembled at either pH 5.0 (a, b) or pH 9.0 (c, d). (Scan size: 1 μm × 1 μm; scan rate: 0.7 μm s^{-1}, scale bar: 0.25 μm).

SPR measurements were used to investigate the adsorption of pFN on terminal layers. FN represents a major ligand for integrin cell adhesion receptors and its adsorption characterizes the potential of biomaterials to interact with cells [7, 11]. Figure 1.6 shows that the adsorption of pFN dissolved in phosphate buffered saline (PBS), pH 7.4, was dependent on the pH value of the PEL solution during PEM assembly. There was no pFN detectable on multilayers formed at acidic conditions, which indicates that no or very limited adsorption of pFN took place. However, on PEM-9 values up to 0.1 ng ml^{-1} pFN were detected with no significant differences between HEP and CHI layer. pFN possesses HEP-binding domains [63, 64] and should enable the protein to adsorb on PEM, particularly when HEP is used as terminal layer. Since HEP seemed to dominate the terminal layer formed at pH 5.0, a high adsorption was expected. However, the apparent absence of pFN adsorption indicates that the orientation or conformation of HEP is unsuitable for interaction with pFN. HEP-binding domains of proteins such as FN require a fitting of segments of HEP molecules into clefts of the protein [64], which would require a loopy or in other way extended conformation of HEP. Due to the strong electrostatic attraction of HEP and diffusion into the multilayer systems, such conformation seems not to be given, which would explain why FN adsorption was so low. Terminal CHI layers formed at pH 5.0 might be also unsuitable because of

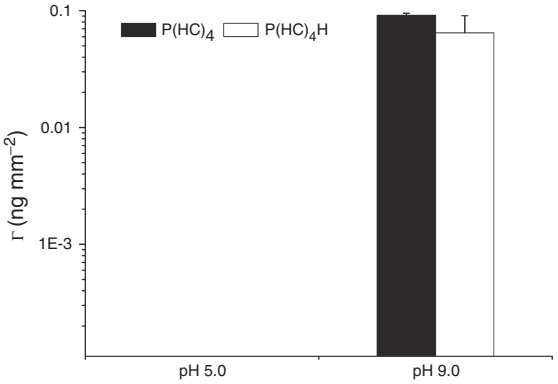

Figure 1.6 Amount of adsorbed pFN on the terminal CHI (black bar) and HEP layer (white bar) assembled at different pH combinations and determined by SPR measurements. The protein was adsorbed with a velocity of 20 µl min^{-1} for 30 min.

their hydrophilicity and the low capability of CHI to adsorb proteins [65, 66]. By contrast, the adsorption of pFN on PEM-9 indicates a more loopy conformation of HEP adsorption due to the weaker interactions with CHI. It is also evident that no difference between terminal HEP and CHI layer exists, which again supports the idea of a more intermingled nature of PEM-9.

MG-63 cells were used to investigate the influence of PEM with different terminating molecules on cell adhesion and growth. First adhesion studies were carried out with scanning electron microscopy (SEM, Quanta 3D FEG, FEI, Frankfurt, Germany) with cells cultured for 4 h in Dulbecco's modified Eagle's medium (DMEM) without serum but preadsorption of 0.5 µg ml^{-1} pFN to allow adhesion of cells, since plain PEM were cytophobic. Figure 1.7 shows clear differences in cell morphology dependent on the pH value and partly the type of terminal layer. First, cells seeded on PEM-5 were strongly polarized (a–d). Second, lamellipodia were present, which points to a motile phenotype of cells. Further, cells on the terminal HEP layer (Figure 1.7c) had a smaller spreading area than cells adherent on the terminal CHI layer (Figure 1.7a). A higher magnification revealed the presence of filopodia, which are used for adhesion to and sensing of the material surface (b, d). An interesting finding was that the edges of the cells were arched, which indicates that cell attachment on these substrata was weaker. Interestingly, a strong difference of cell adhesion dependent on the terminal layer was not found. Cells attached to PEM-9 clearly showed a different behavior. The cells were quite flattened and larger than cells on PEM-5, which indicates a stronger attachment. Again, a clear trend in cell morphology dependent on the terminal layer was not found, which corresponds well to pFN adsorption data.

Quantification of cell adhesion was done by evaluation of phase contrast images of cells (done with Image J) cultured for 4 h in DMEM without serum, but partly with preadsorption of pFN. All PEM exhibited a cytophobic character without

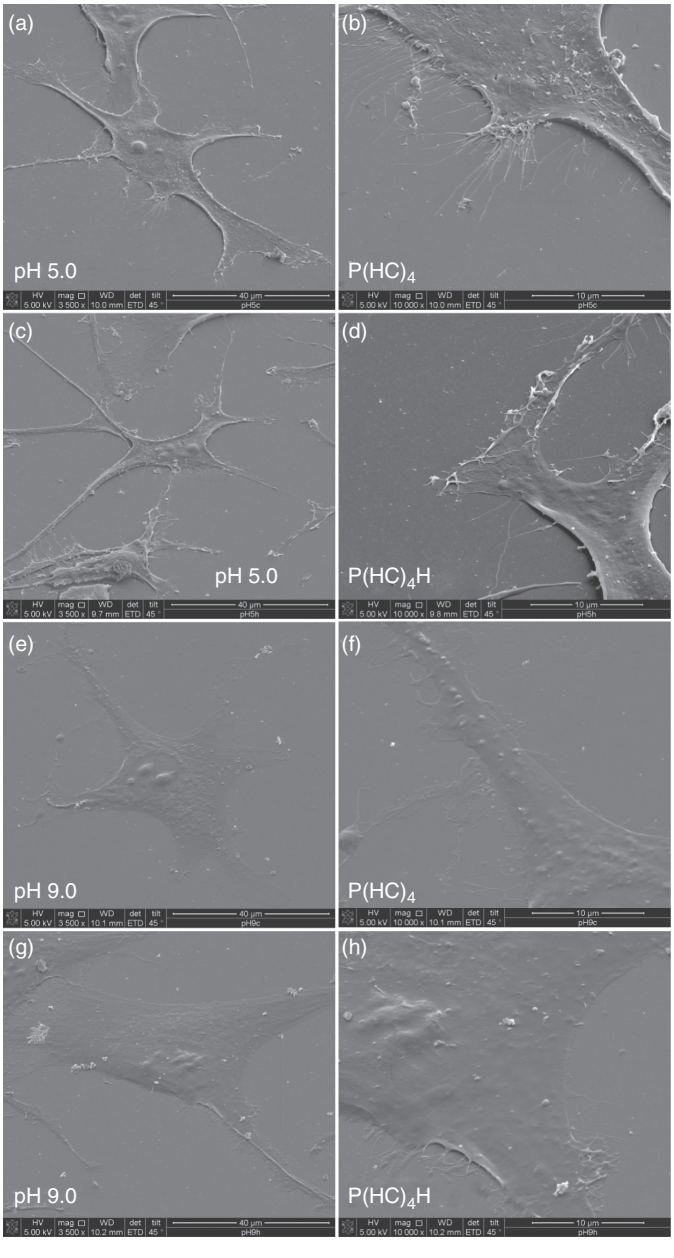

Figure 1.7 SEM images of MG-63 cells at low (left column) and high (right column) magnification and adherent on terminal CHI and HEP layers assembled at pH 5.0 (a–d) and pH 9.0 (e–h) after preadsorption of 0.5 μg ml^{-1} pFN and 4 h incubation in serum-free medium.

pFN preadsorption, which is probably due to the high hydrophilicity of PEM binding water that acts as repulsive barrier for cell adhesion (Figure 1.8a). After preadsorption of 0.5 μg ml^{-1} pFN, a significant increase in cell adhesion was found, which was dependent on pH during multilayer formation. PEM-9, both CHI and HEP, showed the highest cell numbers. For PEM formed at acidic conditions, CHI-terminated showed a higher number of adhering cells than HEP-terminated PEM,

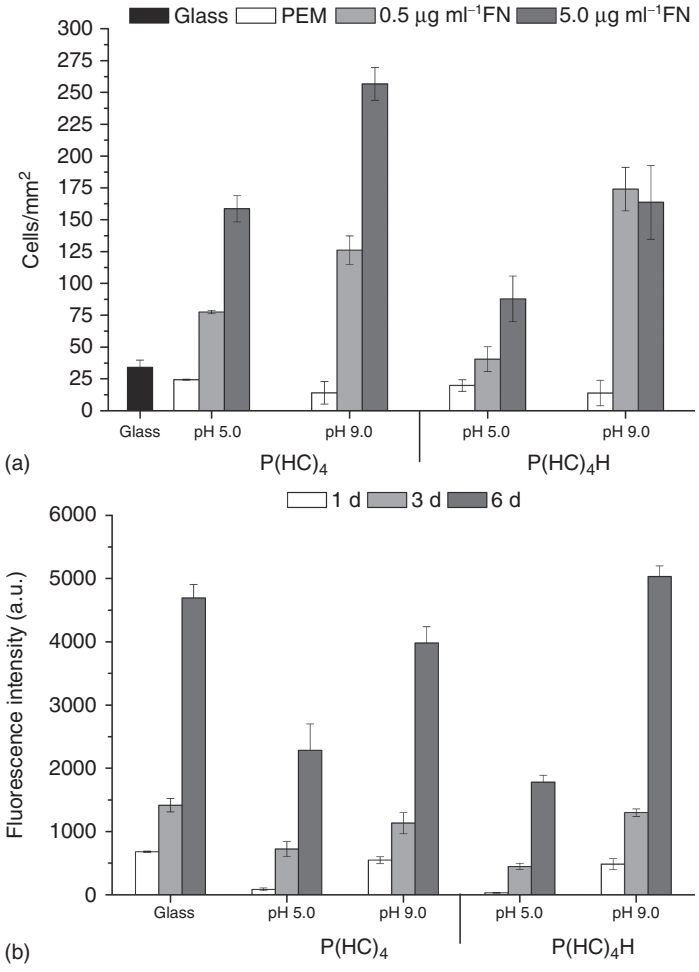

Figure 1.8 Adhesion and growth of MG-63 cells on terminal CHI and HEP layers assembled at pH 5.0 or pH 9.0. (a) The amount of adherent cells to unmodified PEM (white bars) and after preadsorption of 0.5 μg ml^{-1} (light gray bars) or 5.0 μg ml^{-1} (dark gray bars) human pFN in comparison to unmodified glass. Mean values and standard deviations of cells of five images per sample and three independent experiments were calculated. (b) The proliferation of cells over a period of 1 day (white bars), 3 days (light gray bars), and 6 days (dark gray bars) quantified by QBlue metabolic assay of three independent experiments.

but with lower cell numbers than at pH 9.0. After increasing the pFN concentration by 10-fold (5.0 $\mu g\,ml^{-1}$), a rise in cell count was observed. The results of cell adhesion experiments are partly consistent with low pFN adsorption studies, although no pFN adsorption could be detected with SPR on PEM-5. That points to the possibility that minor quantities adsorb also on PEM-5 not detectable by SPR, but effective in interaction with cell adhesion receptors.

The cytophobic character of PEM-5 under protein-free conditions is related to the enhanced hydrophilicity and strong hydration of the GAG, which was proven by WCA and QCM investigations. The adsorption of pFN led to an increase in adhesivity of the PEM dependent on the pFN concentration, which can later be recognized by integrins [7, 67, 68].

Cell proliferation is dependent on protein adsorption as well as cell adhesion and spreading that induce integrin clustering, signal transduction, and activation of mitogen-activated protein (MAP) kinase pathways [69]. Here, we investigated proliferation in the presence of fetal bovine serum (10% FBS in DMEM) without pFN adsorption applying the QBlue® assay, which determines the metabolic activity of cells. Figure 1.8b shows that MG-63 cells were able to adhere initially to the various PEM and to proliferate subsequently over a period of 6 days. HEP-terminated PEM tended to have similar or lower amounts of metabolically active cells than CHI-terminated PEM of the same pH combination. It is also remarkable that the number of metabolically active cells increased with increasing pH during PEM assembly. Further, the proliferation data are in accordance with the adhesion experiments as the interaction of cells with the surface is realized by integrin clustering through outside-in signaling and cell morphology, and actin organization as well as gene expression and migration are influenced [1, 70].

1.2.2 PEI/HEP Multilayers

The system presented here uses HEP as polyanion and PEI as polycation throughout the whole PEM formation process to obtain a system composed of 4.0 or 4.5 bilayers. Both PEL were dissolved in PBS (5.1 mM NaH_2PO_4, 11.7 mM Na_2HPO_4, 140 mM NaCl, pH 7.4) at 2.0 mg ml^{-1}. For the ease of multilayer formation, the pH value during PEM assembly was not further controlled during the initial adsorption steps. The intrinsic pH value of the PEI solution was pH 10.3 ± 0.1, while the pH value of the HEP solution was constant at pH 7.4 ± 0.03. Finally, the pH value was solely adjusted to pH 5.0 (denoted as PEM-5) or pH 9.0 (denoted as PEM-9) for the terminal HEP layer (eighth layer), as in the previous system, to see whether such limited change of condition during the final steps of layer formation would have measurable effect on PEM properties and biological response.

Figure 1.9 shows that the static WCA changed with each PEL adsorption. The polycation always led to a decrease in wettability, whereas the polyanion increased it, which was also seen in the previous study. After adjusting the pH value of HEP solution to either pH 5.0 or 9.0, PEM-5 remained unchanged with low WCA, which was also observed in the HEP/CHI system discussed above, while PEM-9

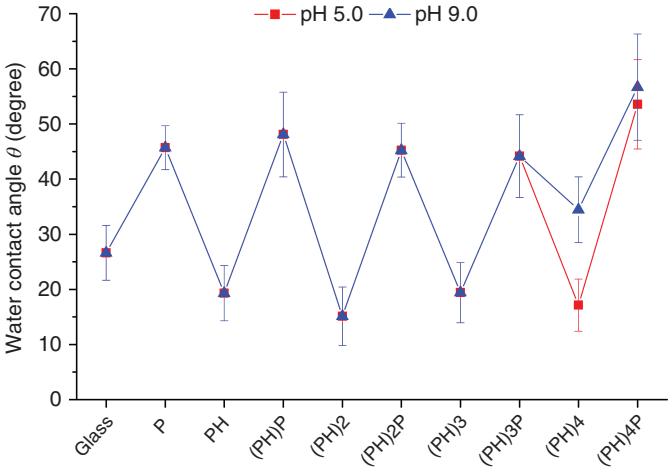

Figure 1.9 Static WCA of PEM consisting of HEP (H) and PEI (P). The pH value of the terminal HEP layer was adjusted to either pH 5.0 (squares) or pH 9.0 (triangles). Mean values and standard deviations of three independent experiments are shown ($n \geq 15$).

had (significantly) higher WCA values. Since PEI has a pK_a of 8.5, it should become less charged upon contact with HEP at pH 9.0, which reduces probably HEP adsorption due to a reduction in ion pairing. However, no significant differences in WCA were observed after adsorption of the last PEI layer, although different quantities of HEP can be expected in the preceding layer.

Zeta potential measurements also revealed a change in PEM composition upon change of the pH value of the HEP solution, but not as expected (Figure 1.10). First, zeta potential of terminal HEP layer followed a sigmoidal trend, which indicates again a contribution of both PEL to the surface potential (Figure 1.10a). Although WCA between PEM-5 and PEM-9 with HEP as terminal layer were different, a significant difference was not found here. Such findings were also made for the HEP/CHI system and indicate that the zeta potential depends not only on the outermost surface but also on the bulk composition of PEM [71]. An additional indicator for this is the PZC, which is located between that of HEP (p$K_a \sim 0.5-1.5$ for sulfate groups; p$K_a \sim 3.0$ for hydroxyl groups) and PEI (p$K_a \sim 8.5$). However, such differences between PEM-5 and PEM-9 were observed for the next PEI layer (Figure 1.10b), although the wetting behavior (WCA) was not different. Zeta potentials of the terminal PEI layers were always positive, but lower at PEM-5 than at PEM-9, especially at higher pH values. This supports the idea that more HEP is present in PEM-5. Due to the contribution of material underneath the terminal layer, it can be sensed here in contrast to WCA measurements. Still, the positive zeta potential of PEI shows that the acidic residues of HEP are efficiently screened, which was also found in similar studies by others [44]. It is interesting to see in later parts of this section that such possibly "hidden" HEP molecules can obviously affect the interaction with cells.

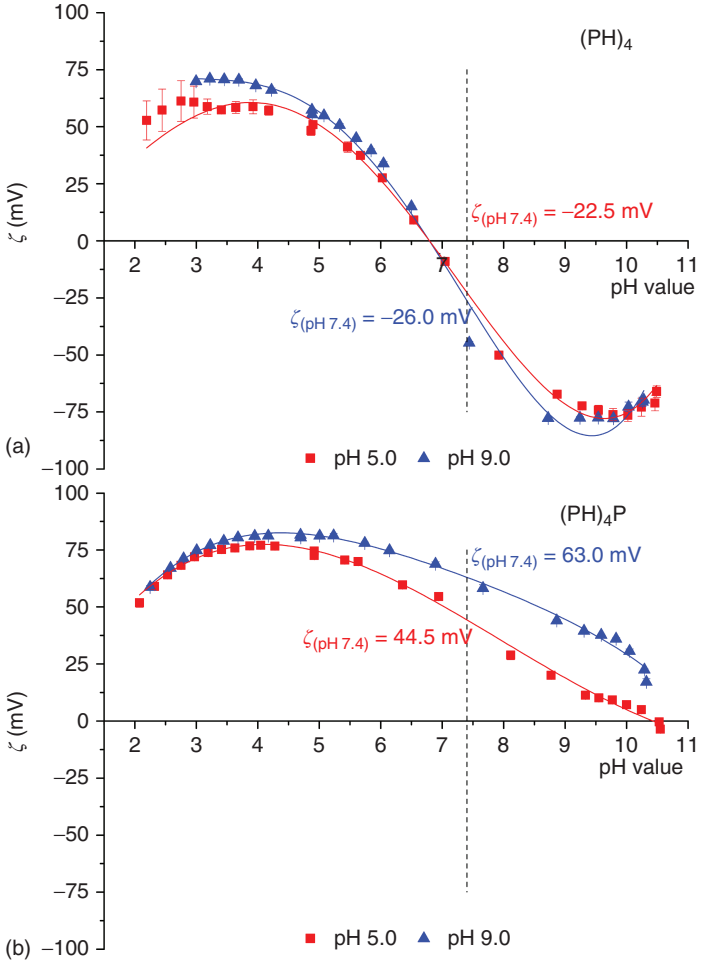

Figure 1.10 Zeta potential titration curves of the terminal HEP (a) and PEI layer (b). The pH value of the terminal HEP layer was adjusted to either pH 5.0 (squares) or pH 9.0 (triangles). Further, the pH value of the buffer solution (1 mM potassium chloride) was titrated from pH 10.0 to pH 3.0 with 1 M hydrochloric acid, and mean values as well as standard deviations of four single measurements were calculated.

The growth of layer mass was measured here with a quartz crystal microbalance with dissipation (QCM-D, QSense, Gothenburg, Sweden). Again, gold sensors were first coated with MUDA to achieve a negative surface charge. An interesting finding was that the total mass increase during the alternating adsorption of HEP and PEI was always higher for the polyanion here, indicated by higher frequency shifts according to Sauerbrey equation [59], which is contrary to the HEP/CHI system (Figure 1.11a). We speculate that the large amount of ionogenic amino groups within the PEI molecule lead to strong ion pairing with HEP. Possibly,

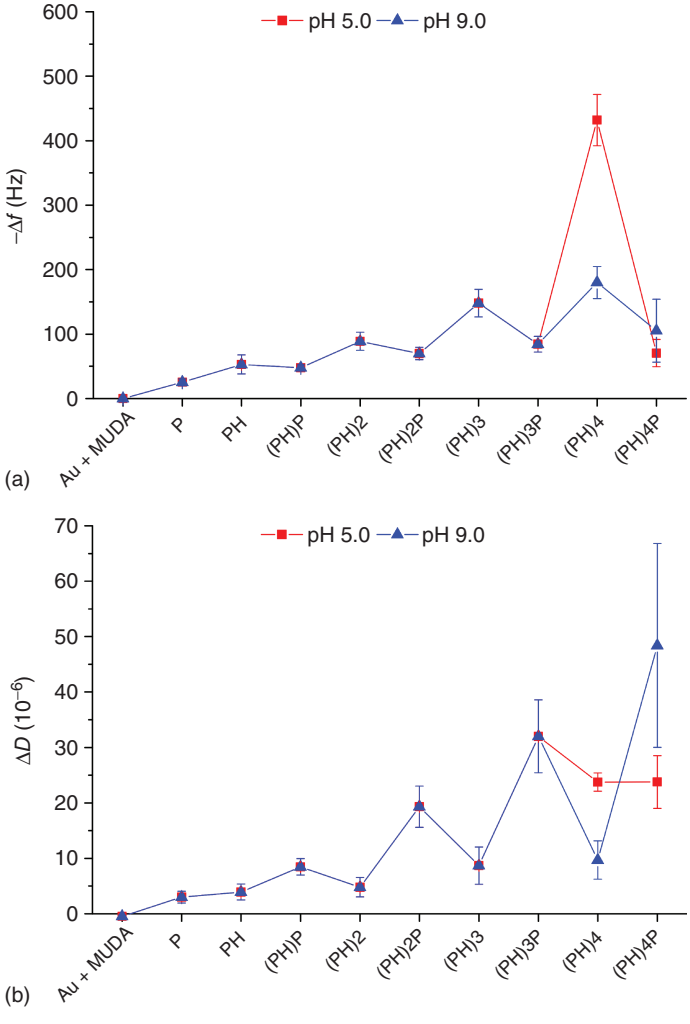

Figure 1.11 QCM-D measurement of PEM growth. Negative frequency shifts Δf (a) as well as the change in dissipation ΔD (b) of HEP (H) and PEI (P) multilayers are shown. The pH value of the terminal HEP layer was adjusted to either pH 5.0 (squares) or pH 9.0 (triangles). Mean values and standard deviations of three independent experiments are indicated.

because of no perfect charge compensation within the PEM system, attraction of water molecules by the charged groups of both PEL is increased that leads to such larger layer mass [61], although PEI is a much larger molecule. This idea is also supported by dissipation measurements shown in Figure 1.11b, where dissipation was always lower for the HEP layers except when pH 5.0 was used during adsorption of the last HEP layer. Conversely, addition of next PEI molecules in solution may drive complexation of previously adsorbed HEP to solution that leads to less

amount of coupled water and lower layer mass. However, a change of pH value of HEP solution for the terminal layer caused a severe shift in frequency, especially at pH 5.0, which points to the fact that much more material is deposited at acidic conditions found also for the HEP/CHI system. It can be assumed that the previous PEI layer becomes highly protonated at pH 5.0, which drives adsorption of more HEP due to a higher match in ion pairing in comparison to pH 9.0 conditions, where hydrogen bonding is favored. Figure 1.11b shows also that more rigid PEM were formed under acidic condition even after addition of PEI that indicates some stable cross-linking of the system due to larger amount of HEP in PEM-5, which was also observed with zeta potential measurements [31, 72]. Higher dissipation values for the polycation layers were also found for the HEP/CHI system and it could indicate that the large polycation PEI is able to entrap large amounts of water, which can be displaced by the smaller molecules such as HEP [31, 43], indicated by a drop in viscoelasticity. However, the high water content was not seen in WCA measurements, which should cause an increase in wettability. Thus, the larger molecule structure of PEI might be the origin of increased viscoelasticity in comparison to the smaller HEP.

The different character of PEM-5 and PEM-9 was also evident by characterization with AFM in hydrated state using a 3D-molecular force probe device (MFP-3D-BIO, Asylum Research, Santa Barbara, USA) (Figure 1.12). Terminal layers of PEM-5 (a, b) were more homogenous than PEM-9 (c, d). Especially, the terminal HEP layer of PEM-9 showed an increase in structure formation that might be attributed to erosion and solution complexation due to the lower electrostatic interaction and increased hydrogen bonding [73]. The high adsorption of HEP at PEM-5, proven by QCM investigations, led to more homogeneous layers due to more flat conformation, which caused highly wettable surfaces, too. Further, the large PEI molecule led to smoother surfaces in comparison to HEP, which was also observed elsewhere [74].

The bioactivity of PEM prepared from HEP and PEI toward cells was studied with human dermal fibroblasts (HDFs). Confocal laser scanning microscopy (CLSM, Leica Microsystems, Wetzlar, Germany) was used to study cell adhesion by visualization of actin cytoskeleton and vinculin in focal adhesions (FAs) after 4 h incubation in DMEM without FBS and preadsorption of 2.0 $\mu g\,ml^{-1}$ pFN. Figure 1.13 shows cell adhesion on PEM assembled at pH 5.0 (a, b) or pH 9.0 (c, d). Even though pFN should specifically bind to HEP due to HEP-binding domains [63, 64], no cells were detected on terminal HEP layers assembled at pH 5.0. This is in line with our previous observations for HEP/CHI PEM-5 and indicates that adsorption of HEP under conditions when ion pairing prevails leads to unfavorable conformation of the molecules for further interactions with proteins [31]. Cells seeded on terminal HEP layers of PEM-9 were slightly spread and polarized with longitudinal actin stress fibers and a large number of shorter FA positive for vinculin. This is also in line with the previous section on HEP/CHI. It demonstrates that adsorption of HEP under conditions when weaker interaction forces such as hydrogen bonding should prevail, its bioactivity is much higher, which is supported by other work published recently [31].

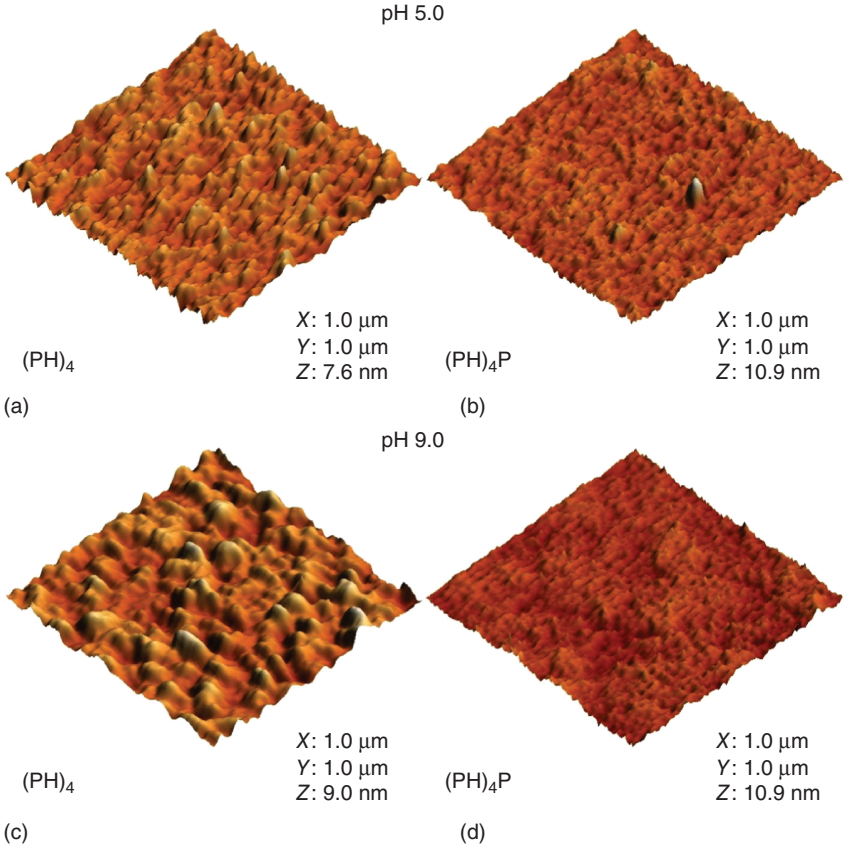

Figure 1.12 AFM images (height profile) of the terminal HEP (a, c) or PEI layer (b, d) in a hydrated state. The pH value of the terminal HEP layer was adjusted to either pH 5.0 (a, b) or pH 9.0 (c, d). (Scan size: 1 µm × 1 µm).

In addition, the wettability and viscoelasticity were reduced at pH 5.0, which is also favorable to cell adhesion [75, 76]. It is interesting to note that adhesion of HDF on terminal PEI layer was also strongly affected by pH during PEM assembly. Here, spreading and FA formation was high on PEI at PEM-5, whereas cell death was indicated by the appearance of cells on PEI at PEM-9. In general, positively charged surfaces are more attractive for protein adsorption and cell adhesion [77], which explains the good attachment of cells on terminal PEI layers. The lower cytotoxicity of terminal PEI layers in PEM-5 indicates some intermingling with HEP that seems to reduce the toxic effect of the polycation.

Qualitative cell adhesion studies were succeeded by quantification of the amount of metabolically active cells using the QBlue® assay after culturing the cells for 4 h with or without preadsorption of 2.0 µg ml^{-1} pFN in the absence of serum

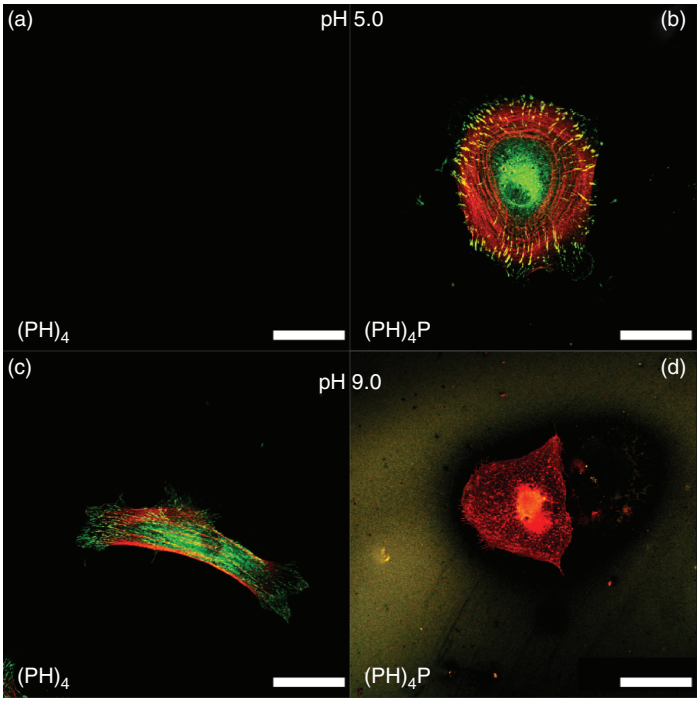

Figure 1.13 CLSM images of HDF adherent on terminal layers of HEP (a, c) and PEI (b, d) at pH 5.0 (a, b) or pH 9.0 (c, d) after preadsorption of 2.0 μg ml^{-1} pFN and 4 h incubation in serum-free medium. The cells were stained for filamentous actin (red) and vinculin in focal adhesion plaques (green). (Scale: 50 μm)

proteins. It was found that that all PEM exhibited cytophobic character without pFN preadsorption independent of the pH value (Figure 1.14a). However, it can be seen that the adsorption of pFN had a promoting, but not significant, effect on cell adhesion on all PEM, except on PEI in PEM-5, where less metabolically active cells were found. Nevertheless, here actin was organized in bundles circumferentially and vinculin present in FA and cells in the CLSM images did appear metabolically active in comparison to pH 9.0. The improved adhesion on PEI of PEM-5 might be attributed to the viscoelasticity, since no differences in wettability were found and the zeta potential was lower in PEM-5. Further, HEP that could be intermingled with PEI, as indicated by the lower zeta potential, might allow specific interaction with pFN supporting cell adhesion. The hampered spreading of HDF at alkaline conditions indicated that PEI exerted a certain cytotoxicity [78] due to high PEI concentration supported by higher zeta potentials of PEM-9.

Proliferation of HDF was monitored again with the QBlue® assay over a period of 7 days (Figure 1.14b). In the presence of 10% FBS containing adhesive proteins with HEP-binding domains such as FN and vitronectin [79], cells were able to adhere initially to the various PEM and to proliferate subsequently. The amount of metabolically active cells was always lower on HEP-terminated in comparison

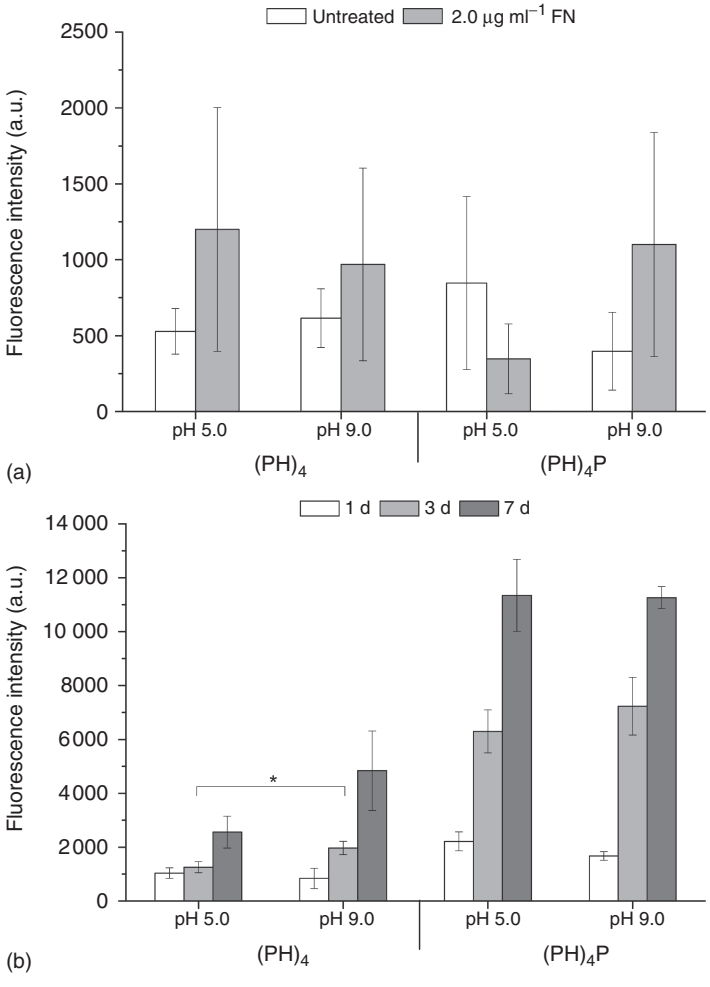

Figure 1.14 Adhesion and growth of HDF on terminal HEP and PEI layers assembled at pH 5.0 or pH 9.0. (a) The amount of metabolically active cells on unmodified PEM (white bars) and after preadsorption of 2.0 μg ml^{-1} human pFN (gray bars). Mean values and standard deviations of three independent experiments are indicated. (b) The proliferation of cells over a period of 1 day (white bars), 3 days (light gray bars), and 7 days (dark gray bars) quantified by QBlue metabolic assay. Differences were analyzed by ANOVA and *post hoc* Tukey testing (*$p < 0.05$).

to PEI-terminated PEM. The presence of serum reduced obviously the cytotoxic effect of PEI [28] in terminal layers of PEM-9 and diminished the differences found under serum-free conditions during adhesion studies. Further, the impact of FBS was stronger on PEI in comparison to HEP layers. It can be assumed here that the positive zeta potential under physiological conditions leads to much higher adsorption of proteins [80]. It is interesting to note that the number

of metabolically active cells increased with increasing pH on HEP-terminated PEM, which was also found during the cell adhesion studies. Moreover, this phenomenon was also observed for the HEP/CHI system described before. Overall, the data show that also with the use of HEP and PEI as PEL, a multilayer system can be established that allows regulation of cell adhesion and growth by changes of pH value during layer assembly. It is remarkable that a change of pH during the final steps of PEM formation has such strong effect, which we showed also in a recent paper for the CHI/HEP system [31].

1.3 Summary and Outlook

The studies presented here show how a change of pH value during PEL complexation from conditions when ion pairing should prevail to when most probably hydrogen bonding becomes dominating influence multilayer wetting properties, partly zeta potential, multilayer mass, and viscoelastic properties and with that adhesion and growth of cells. Besides, the use of a simple parameter such as pH value to change multilayer properties, also the choice of molecules, being either biogenic or synthetic, contributes to the value of this study. HEP as GAG has an inherent bioactivity by its ability to interact with a plethora of different proteins that regulate adhesion, growth, and differentiation of cells [41]. Hence, multilayers composed of HEP are potential candidates to be reservoirs for proteins such as FN, bone morphogenic proteins (BMPs), and other growth factors that regulate adhesion, homing, and differentiation of cells or chemokines such as stromal cell-derived factor 1 (SDF-1) that attract stem cells [81–83]. CHI, on the other hand, does not only represent a simple building block because of its cationic nature at acidic pH values, but has inherent antibacterial, antifungal, and anti-inflammatory properties [42]. In addition, the use of PEI as polycation bears the potential to use multilayers for complexation with DNA and as *in situ* transfection system for coating implant materials and tissue engineering scaffolds [84, 85].

As it was shown in this study, adhesion and growth of two different cell types such as MG-63 osteosarcoma cells and primary fibroblasts could be regulated by the conditions applied during multilayer formation and the dominating molecule in the terminal layer. This not only enables to support or block cell adhesion but also could be used by more subtle changes of pH value during multilayer formation [35, 43] to regulate adhesion and spreading of cells. It is interesting to note that cell spreading has different effect on cells from epithelial and mesenchymal origin, which is also important for their function [11, 86, 87]. Since cell spreading is related to signal transduction [2, 88], degree of cell spreading on material surfaces is a tool to control cell functions and with that, the outcome of application of implants and tissue engineering scaffolds. Because of its ease and application of fluids that also wet materials with sophisticated shape and inner porosity, the LbL technique is a versatile tool to adapt biomaterials to specific medical applications.

Acknowledgments

This work was supported partly by the German Academic Exchange Service (DAAD) in the frame of a bilateral exchange program between Germany and Bulgaria (Prof. G. Altankov) as well as Germany and Greece (Prof. Y. Missirlis). KK and MSN are grateful for scholarships from the DAAD. The authors thank the German Research Society (DFG) for financial support through Grant GR 1290/10-1.

References

1. Hynes, R.O. (2002) Integrins: bidirectional, allosteric signaling machines. *Cell*, **110**, 673–687.
2. Giancotti, F.G. and Ruoslahti, E. (1999) Integrin signaling. *Science*, **285**, 1028–1033.
3. Curtis, A.S., Forrester, J.V., McInnes, C., and Lawrie, F. (1983) Adhesion of cells to polystyrene surfaces. *J. Cell Biol.*, **97**, 1500–1506.
4. Grinnell, F. and Feld, M.K. (1979) Initial adhesion of human fibroblasts in serum-free medium: possible role of secreted fibronectin. *Cell*, **17**, 117–129.
5. Trommler, A., Gingell, D., and Wolf, H. (1985) Red blood-cells experience electrostatic repulsion but make molecular adhesions with glass. *Biophys. J.*, **48**, 835–841.
6. Altankov, G., Richau, K., and Groth, T. (2003) The role of surface zeta potential and substratum chemistry for regulation of dermal fibroblasts interaction. *Materialwiss. Werkstofftech.*, **34**, 1120–1128.
7. Faucheux, N., Schweiss, R., Lutzow, K., Werner, C., and Groth, T. (2004) Self-assembled monolayers with different terminating groups as model substrates for cell adhesion studies. *Biomaterials*, **25**, 2721–2730.
8. Keselowsky, B.G., Collard, D.M., and Garcia, A.J. (2003) Surface chemistry modulates fibronectin conformation and directs integrin binding and specificity to control cell adhesion. *J. Biomed. Mater. Res. A*, **66A**, 247–259.
9. Altankov, G., Grinnell, F., and Groth, T. (1996) Studies on the biocompatibility of materials: fibroblast reorganization of substratum-bound fibronectin on surfaces varying in wettability. *J. Biomed. Mater. Res.*, **30**, 385–391.
10. Salmeron-Sanchez, M., Rico, P., Moratal, D., Lee, T.T., Schwarzbauer, J.E., and Garcia, A.J. (2011) Role of material-driven fibronectin fibrillogenesis in cell differentiation. *Biomaterials*, **32**, 2099–2105.
11. Tzoneva, R., Groth, T., Altankov, G., and Paul, D. (2002) Remodeling of fibrinogen by endothelial cells in dependence on fibronectin matrix assembly. Effect of substratum wettability. *J. Mater. Sci.: Mater. Med.*, **13**, 1235–1244.
12. Decher, G. and Schlenoff, J.B. (2012) in *Multilayer Thin Films: Sequential Assembly of Nanocomposite Materials* (eds G. Decher and J.B. Schlenoff), Wiley-VCH Verlag GmbH, vol. 1, pp. 1–320.
13. Quinn, J.F., Johnston, A.P.R., Such, G.K., Zelikin, A.N., and Caruso, F. (2007) Next generation, sequentially assembled ultrathin films: beyond electrostatics. *Chem. Soc. Rev.*, **36**, 707–718.
14. Mhamdi, L., Picart, C., Lagneau, C., Othmane, A., Grosgogeat, B., Jaffrezic-Renault, N., and Ponsonnet, L. (2006) Study of the polyelectrolyte multilayer thin films' properties and correlation with the behavior of the human gingival fibroblasts. *Mater. Sci. Eng., C: Biomimetic Supramol. Syst.*, **26**, 273–281.
15. Picart, C., Gergely, C., Arntz, Y., Voegel, J.-C., Schaaf, P., Cuisinier, F.J.G., and Senger, B. (2004) Measurement of film thickness up to several hundreds of nanometers using optical waveguide lightmode spectroscopy. *Biosens. Bioelectron.*, **20**, 553–561.

16. Mendelsohn, J.D., Barrett, C.J., Chan, V.V., Pal, A.J., Mayes, A.M., and Rubner, M.F. (2000) Fabrication of microporous thin films from polyelectrolyte multilayers. *Langmuir*, **16**, 5017–5023.
17. Shiratori, S.S. and Rubner, M.F. (2000) pH-dependent thickness behavior of sequentially adsorbed layers of weak polyelectrolytes. *Macromolecules*, **33**, 4213–4219.
18. Yoo, D., Shiratori, S.S., and Rubner, M.F. (1998) Controlling bilayer composition and surface wettability of sequentially adsorbed multilayers of weak polyelectrolytes. *Macromolecules*, **31**, 4309–4318.
19. Thompson, M.T., Berg, M.C., Tobias, I.S., Rubner, M.F., and Van Vliet, K.J. (2005) Tuning compliance of nanoscale polyelectrolyte multilayers to modulate cell adhesion. *Biomaterials*, **26**, 6836–6845.
20. Ngankam, A.P., Mao, G.Z., and Van Tassel, P.R. (2004) Fibronectin adsorption onto polyelectrolyte multilayer films. *Langmuir*, **20**, 3362–3370.
21. Mendelsohn, J.D., Yang, S.Y., Hiller, J., Hochbaum, A.I., and Rubner, M.F. (2003) Rational design of cytophilic and cytophobic polyelectrolyte multilayer thin films. *Biomacromolecules*, **4**, 96–106.
22. Salloum, D.S. and Schlenoff, J.B. (2004) Protein adsorption modalities on polyelectrolyte multilayers. *Biomacromolecules*, **5**, 1089–1096.
23. Zhang, J., Senger, B., Vautier, D., Picart, C., Schaaf, P., Voegel, J.C., and Lavalle, P. (2005) Natural polyelectrolyte films based on layer-by layer deposition of collagen and hyaluronic acid. *Biomaterials*, **26**, 3353–3361.
24. Grohmann, S., Rothe, H., Frant, M., and Liefeith, K. (2011) Colloidal force spectroscopy and cell biological investigations on biomimetic polyelectrolyte multilayer coatings composed of chondroitin sulfate and heparin. *Biomacromolecules*, **12**, 1987–1997.
25. Mhanna, R.F., Vörös, J., and Zenobi-Wong, M. (2011) Layer-by-layer films made from extracellular matrix macromolecules on silicone substrates. *Biomacromolecules*, **12**, 609–616.
26. Cai, K.Y., Rechtenbach, A., Hao, J.Y., Bossert, J., and Jandt, K.D. (2005) Polysaccharide-protein surface modification of titanium via a layer-by-layer technique: characterization and cell behaviour aspects. *Biomaterials*, **26**, 5960–5971.
27. Lundin, M., Solaqa, F., Thormann, E., Macakova, L., and Blomberg, E. (2011) Layer-by-layer assemblies of chitosan and heparin: effect of solution ionic strength and pH. *Langmuir*, **27**, 7537–7548.
28. Niepel, M.S., Peschel, D., Sisquella, X., Planell, J.A., and Groth, T. (2009) pH-dependent modulation of fibroblast adhesion on multilayers composed of poly(ethylene imine) and heparin. *Biomaterials*, **30**, 4939–4947.
29. Boudou, T., Crouzier, T., Nicolas, C., Ren, K., and Picart, C. (2011) Polyelectrolyte multilayer nanofilms used as thin materials for cell mechano-sensitivity studies. *Macromol. Biosci.*, **11**, 77–89.
30. Liu, Z.-M., Gu, Q., Xu, Z.-K., and Groth, T. (2010) Synergistic effect of polyelectrolyte multilayers and osteogenic growth medium on differentiation of human mesenchymal stem cells. *Macromol. Biosci.*, **10**, 1043–1054.
31. Aggarwal, N., Altgarde, N., Svedhem, S., Michanetzis, G., Missirlis, Y., and Groth, T. (2013) Tuning cell adhesion and growth on biomimetic polyelectrolyte multilayers by variation of pH during layer-by-layer assembly. *Macromol. Biosci.*, **13**, 1327–1338.
32. Kirchhof, K., Hristova, K., Krasteva, N., Altankov, G., and Groth, T. (2009) Multilayer coatings on biomaterials for control of MG-63 osteoblast adhesion and growth. *J. Mater. Sci.: Mater. Med.*, **20**, 897–907.
33. Richert, L., Arntz, Y., Schaaf, P., Voegel, J.C., and Picart, C. (2004) pH dependent growth of poly(L-lysine)/poly(L-glutamic) acid multilayer films and their cell adhesion properties. *Surf. Sci.*, **570**, 13–29.
34. Koewitsch, A., Yang, Y., Ma, N., Kuntsche, J., Mader, K., and Groth, T. (2011) Bioactivity of immobilized hyaluronic acid derivatives regarding

protein adsorption and cell adhesion. *Biotechnol. Appl. Biochem.*, **58**, 376–389.
35. Boddohi, S., Killingsworth, C.E., and Kipper, M.J. (2008) Polyelectrolyte multilayer assembly as a function of pH and ionic strength using the polysaccharides chitosan and heparin. *Biomacromolecules*, **9**, 2021–2028.
36. Lavalle, P., Picart, C., Mutterer, J., Gergely, C., Reiss, H., Voegel, J.-C., Senger, B., and Schaaf, P. (2003) Modeling the buildup of polyelectrolyte multilayer films having exponential growth. *J. Phys. Chem. B*, **108**, 635–648.
37. Richert, L., Lavalle, P., Payan, E., Shu, X.Z., Prestwich, G.D., Stoltz, J.F., Schaaf, P., Voegel, J.C., and Picart, C. (2004) Layer by layer buildup of polysaccharide films: physical chemistry and cellular adhesion aspects. *Langmuir*, **20**, 448–458.
38. Burke, S.E. and Barrett, C.J. (2003) pH-responsive properties of multilayered poly(L-lysine)/hyaluronic acid surfaces. *Biomacromolecules*, **4**, 1773–1783.
39. Xie, A.F. and Granick, S. (2001) Weak versus strong: a weak polyacid embedded within a multilayer of strong polyelectrolytes. *J. Am. Chem. Soc.*, **123**, 3175–3176.
40. Crouzier, T., Boudou, T., and Picart, C. (2010) Polysaccharide-based polyelectrolyte multilayers. *Curr. Opin. Colloid Interface Sci.*, **15**, 417–426.
41. Capila, I. and Linhardt, R.J. (2002) Heparin – protein interactions. *Angew. Chem. Int. Ed.*, **41**, 391–412.
42. Di Martino, A., Sittinger, M., and Risbud, M.V. (2005) Chitosan: a versatile biopolymer for orthopaedic tissue-engineering. *Biomaterials*, **26**, 5983–5990.
43. Kirchhof, K. (2010) Nanostrukturierte Biomaterialbeschichtungen zur Steuerung von Zelladhäsion und -proliferation pH-Wert-abhängige Multischichten aus Heparin und Chitosan in diskreter und Gradientenform. Dissertation. Martin Luther University Halle-Wittenberg, published in Shaker Verlag GmbH, ISBN: 978-3-8322-9041-2, p. 160.
44. Schoenhoff, M. (2003) Layered polyelectrolyte complexes: physics of formation and molecular properties. *J. Phys. Condens. Matter*, **15**, R1781–R1808.
45. Bain, C.D. and Whitesides, G.M. (1988) Depth sensitivity of wetting: monolayers of. omega.-mercapto ethers on gold. *J. Am. Chem. Soc.*, **110**, 5897–5898.
46. Leceta, I., Guerrero, P., and de la Caba, K. (2013) Functional properties of chitosan-based films. *Carbohydr. Polym.*, **93**, 339–346.
47. Mota, R.P., Perrenoud, I.A., Honda, R.Y., Algatti, M.A., Kayama, M.E., Kostov, K.G., Sadahito China, T., and Cruz, N.C. (2012) Biocompatible thin films obtained from heparin-methane plasma process. Proceedings of the 13th International Conference on Plasma Surface Engineering.
48. Kang, H.-S., Park, S.-H., Lee, Y.-G., and Son, T.-I. (2007) Polyelectrolyte complex hydrogel composed of chitosan and poly(γ-glutamic acid) for biological application: preparation, physical properties, and cytocompatibility. *J. Appl. Polym. Sci.*, **103**, 386–394.
49. Schlenoff, J.B. and Dubas, S.T. (2001) Mechanism of polyelectrolyte multilayer growth: charge overcompensation and distribution. *Macromolecules*, **34**, 592–598.
50. Dong, P., Hao, W.C., Xia, Y.Y., Da, G.Z., and Wang, T.M. (2010) Comparison study of corrosion behavior and biocompatibility of polyethyleneimine (PET)/heparin and chitosan/heparin coatings on NiTi alloy. *J. Mater. Sci. Technol.*, **26**, 1027–1031.
51. Holmesfarley, S.R., Bain, C.D., and Whitesides, G.M. (1988) Wetting of functionalized polyethylene film having ionizable organic-acids and bases at the polymer water interface – relations between functional-group polarity, extent of ionization, and contact-angle with water. *Langmuir*, **4**, 921–937.
52. Salmivirta, M., Lidholt, K., and Lindahl, U. (1996) Heparan sulfate: a piece of information. *FASEB J.: Off. Publ. Fed. Am. Soc. Exp. Biol.*, **10**, 1270–1279.
53. Liu, Y.J., Navasero, N.M., and Yu, H.Z. (2004) Structure and reactivity of mixed omega-carboxyalkyl/alkyl monolayers on silicon: ATR-FTIR spectroscopy and

contact angle titration. *Langmuir*, **20**, 4039–4050.
54. Zimmermann, R. (2004) Charakterisierung von Ladungsbildungsprozessen an Polymeren in wässrigen Lösungen. Dissertation, web Universitätsverlag.
55. Ladam, G., Schaad, P., Voegel, J.C., Schaaf, P., Decher, G., and Cuisinier, F. (2000) In situ determination of the structural properties of initially deposited polyelectrolyte multilayers. *Langmuir*, **16**, 1249–1255.
56. Richert, L., Boulmedais, F., Lavalle, P., Mutterer, J., Ferreux, E., Decher, G., Schaaf, P., Voegel, J.C., and Picart, C. (2004) Improvement of stability and cell adhesion properties of polyelectrolyte multilayer films by chemical cross-linking. *Biomacromolecules*, **5**, 284–294.
57. Duval, J.F.L., KÜttner, D., Werner, C., and Zimmermann, R. (2011) Electrohydrodynamics of soft polyelectrolyte multilayers: point of zero-streaming current. *Langmuir*, **27**, 10739–10752.
58. Richert, L., Lavalle, P., Vautier, D., Senger, B., Stoltz, J.F., Schaaf, P., Voegel, J.C., and Picart, C. (2002) Cell interactions with polyelectrolyte multilayer films. *Biomacromolecules*, **3**, 1170–1178.
59. Sauerbrey, G. (1959) Verwendung von Schwingquarzen zur Wägung dünner Schichten und zur MikrowÃ¤gung. *Z. Phys. A: Hadrons Nucl.*, **155**, 206–222.
60. Kujawa, P., Moraille, P., Sanchez, J., Badia, A., and Winnik, F.M. (2005) Effect of molecular weight on the exponential growth and morphology of hyaluronan/chitosan multilayers: a surface plasmon resonance spectroscopy and atomic force microscopy investigation. *J. Am. Chem. Soc.*, **127**, 9224–9234.
61. Crouzier, T. and Picart, C. (2009) Ion pairing and hydration in polyelectrolyte multilayer films containing polysaccharides. *Biomacromolecules*, **10**, 433–442.
62. Picart, C. (2008) Polyelectrolyte multilayer films: from physico-chemical properties to the control of cellular processes. *Curr. Med. Chem.*, **15**, 685–697.
63. Casu, B. (1994) Protein-binding domains of heparin and other sulfated glycosaminoglycans. *Carbohydr. Eur.*, **11**, 18–21.
64. Pankov, R. and Yamada, K.M. (2002) Fibronectin at a glance. *J. Cell Sci.*, **115**, 3861–3863.
65. Croll, T.I., O'Connor, A.J., Stevens, G.W., and Cooper-White, J.J. (2006) A blank slate? Layer-by-layer deposition of hyaluronic acid and chitosan onto various surfaces. *Biomacromolecules*, **7**, 1610–1622.
66. Hoven, V.P., Tangpasuthadol, V., Angkitpaiboon, Y., Vallapa, N., and Kiatkamjornwong, S. (2007) Surface-charged chitosan: preparation and protein adsorption. *Carbohydr. Polym.*, **68**, 44–53.
67. Altankov, G. and Groth, T. (1996) Fibronectin matrix formation and the biocompatibility of materials. *J. Mater. Sci.: Mater. Med.*, **7**, 425–429.
68. Keselowsky, B.G., Collard, D.M., and Garcia, A.J. (2004) Surface chemistry modulates focal adhesion composition and signaling through changes in integrin binding. *Biomaterials*, **25**, 5947–5954.
69. Wozniak, M.A., Modzelewska, K., Kwong, L., and Keely, P.J. (2004) Focal adhesion regulation of cell behavior. *Biochim. Biophys. Acta, Mol. Cell. Res.*, **1692**, 103–119.
70. Ruoslahti, E. (1997) Integrins as signaling molecules and targets for tumor therapy. *Kidney Int.*, **51**, 1413–1417.
71. Dukhin, S.S., Zimmermann, R., and Werner, C. (2008) Charge density distribution at interfaces between polyelectrolyte layers and aqueous solutions–experimental access and limitations of traditional electrokinetics. *J. Colloid Interface Sci.*, **328**, 217–226.
72. Notley, S.M., Eriksson, M., and Wagberg, L. (2005) Visco-elastic and adhesive properties of adsorbed polyelectrolyte multilayers determined in situ with QCM-D and AFM measurements. *J. Colloid Interface Sci.*, **292**, 29–37.
73. Aggarwal, N., Altgarde, N., Svedhem, S., Zhang, K., Fischer, S., and Groth, T. (2013) Effect of molecular composition of heparin and cellulose sulfate on multilayer formation and cell response. *Langmuir*, **29**, 13853–13864.
74. Trimpert, C., Boese, G., Albrecht, W., Richau, K., Weigel, T., Lendlein, A.,

and Groth, T. (2006) Poly(ether imide) membranes modified with poly(ethylene imine) as potential carriers for epidermal substitutes. *Macromol. Biosci.*, **6**, 274–284.

75. Pelham, R.J. and Wang, Y.L. (1998) Cell locomotion and focal adhesions are regulated by substrate flexibility (vol 94, pg 13661, 1997). *Proc. Natl. Acad. Sci. U.S.A.*, **95**, 12070.
76. Tzoneva, R., Faucheux, N., and Groth, T. (2007) Wettability of substrata controls cell-substrate and cell-cell adhesions. *Biochim. Biophys. Acta, Gen. Subj.*, **1770**, 1538–1547.
77. Muller, M., Rieser, T., Dubin, P.L., and Lunkwitz, K. (2001) Selective interaction between proteins and the outermost surface of polyelectrolyte multilayers: influence of the polyanion type, pH and salt. *Macromol. Rapid Commun.*, **22**, 390–395.
78. Brunot, C., Ponsonnet, L., Lagneau, C., Farge, P., Picart, C., and Grosgogeat, B. (2007) Cytotoxicity of polyethyleneimine (PEI), precursor base layer of polyelectrolyte multilayer films. *Biomaterials*, **28**, 632–640.
79. Dalton, B.A., McFarland, C.D., Underwood, P.A., and Steele, J.G. (1995) Role of the heparin binding domain of fibronectin in attachment and spreading of human bone-derived cells. *J. Cell Sci.*, **108**, 2083–2092.
80. Norde, W. and Lyklema, J. (1991) Why proteins prefer interfaces. *J. Biomater. Sci. Polym. Ed.*, **2**, 183–202.
81. Crouzier, T., Ren, K., Nicolas, C., Roy, C., and Picart, C. (2009) Layer-by-layer films as a biomimetic reservoir for rhBMP-2 delivery: controlled differentiation of myoblasts to osteoblasts. *Small*, **5**, 598–608.
82. Crouzier, T., Sailhan, F., Becquart, P., Guillot, R., Logeart-Avramoglou, D., and Picart, C. (2011) The performance of BMP-2 loaded TCP/HAP porous ceramics with a polyelectrolyte multilayer film coating. *Biomaterials*, **32**, 7543–7554.
83. Goncalves, R.M., Antunes, J.C., and Barbosa, M.A. (2012) Mesenchymal stem cell recruitment by stromal derived factor-1-delivery systems based on chitosan/poly(gamma-glutamic acid) polyelectrolyte complexes. *Eur. Cell. Mater.*, **23**, 249–260; discussion 260–261.
84. Mehrotra, S., Lee, I., and Chan, C. (2009) Multilayer mediated forward and patterned siRNA transfection using linear-PEI at extended N/P ratios. *Acta Biomater.*, **5**, 1474–1488.
85. Sun, J.-K., Ren, K.-F., and Ji, J. (2012) pH-triggered DNA delivery based on multilayer film of DNA polyplexes and charge-reversible poly(ethylenimine). *Thin Solid Films*, **520**, 5426–5430.
86. Boese, G., Trimpert, C., Albrecht, W., Malsch, G., Groth, T., and Lendlein, A. (2007) Membranes from acrylonitrile-based polymers for selective cultivation of human keratinocytes. *Tissue Eng.*, **13**, 2995–3002.
87. Ryan, P.L., Foty, R.A., Kohn, J., and Steinberg, M.S. (2001) Tissue spreading on implantable substrates is a competitive outcome of cell-cell vs. cell-substratum adhesivity. *Proc. Natl. Acad. Sci. U.S.A.*, **98**, 4323–4327.
88. Müller, P., Langenbach, A., Kaminski, A., and Rychly, J. (2013) Modulating the actin cytoskeleton affects mechanically induced signal transduction and differentiation in mesenchymal stem cells. *PLoS One*, **8**, e71283.